Smartphone-Based Point-of-Care Urinalysis Under Variable Illumination

**MOONSOO RA[1], MANNAN SAEED MUHAMMAD[2], (Member, IEEE), CHIAWEI LIM[1,3],
SEHUI HAN[1,4], CHANSUNG JUNG[5], AND WHOI-YUL KIM[6], (Member, IEEE)**

[1]Department of Electronics and Computer Engineering, Hanyang University, Seoul 04763, South Korea
[2]School of Electronic and Electrical Engineering, College of Information and Communication, Sungkyunkwan University, Suwon 16419, South Korea
[3]Skymind Corporation, San Francisco, CA 94103, USA
[4]LG Electronics, Pyeongteak 177709, South Korea
[5]Department of Intelligent Robot Engineering, Hanyang University, Seoul 04763, South Korea
[6]Department of Electronic Engineering, Hanyang University, Seoul 04763, South Korea

CORRESPONDING AUTHOR: W.-Y. KIM (wykim@hanyang.ac.kr)

ABSTRACT Urine tests are performed by using an off-the-shelf reference sheet to compare the color of test strips. However, the tabular representation is difficult to use and more prone to visual errors, especially when the reference color-swatches to be compared are spatially apart. Thus, making it is difficult to distinguish between the subtle differences of shades on the reagent pads. This manuscript represents a new arrangement of reference arrays for urine test strips (urinalysis). Reference color swatches are grouped in a doughnut chart, surrounding each reagent pad on the strip. The urine test can be evaluated using naked eye by referring to the strip with no additional sheet necessary. Along with this new strip, an algorithm for smartphone based application is also proposed as an alternative to deliver diagnostic results. The proposed colorimetric detection method evaluates the captured image of the strip, under various color spaces and evaluates ten different tests for urine. Thus, the proposed system can deliver results on the spot using both naked eye and smartphone. The proposed scheme delivered accurate results under various environmental illumination conditions without any calibration requirements, exhibiting performances suitable for real-life applications and an ease for a common user.

INDEX TERMS Smartphone, colorimetric, optical sensor, point-of-care, diagnostics, color-matching, urinalysis.

I. INTRODUCTION

Point of Care Testing (POCT), [1]–[8], has been gaining attention for its wide applications in public health. Ranging from blood glucose measurement to complex immunological assays, POCT is simple to use even for end users with little technical expertise. This characteristic makes it particularly suitable for disease detection, quality of care, or patient compliance monitoring. Although, advancements in semiconductor technology have helped create transformative consumer devices, but so far, have limited impact on the medical world. Medical devices have stringent requirements for safety and effectiveness, and they generally iterate on bulky, power-hungry designs. One of the leading diagnostic tools of POCT analysis is strip-based colorimetric diagnostic assays. When samples such as urine, blood, or other body fluids are deposited on a test strip, signals are obtained in the form of colors. Evaluation of the changes in colors, which is done by simple human perception, is generally accurate. However, the colors may be perceived differently due to varying light conditions, resulting in diagnostic errors which are likely to affect the medical decision-making of users, [9].

To reduce human errors, some technology devices to assist the interpretation of the diagnostic results have been introduced. Digital photography, digital scanners, and smartphones have been utilized to study the effects of light and colors on the chemistry of solutions, [10]–[14]. In health care products, device portable colorimetric readers [15], scanners [10], video cameras [16], or high-resolution digital cameras [17], have been deployed to capture the colorimetric data as digital images. In these works, mostly, a sample holder is used to fixate a paper-based microfluidic plastic substrate and also the surrounding light effects are removed. The color of the reagent pads on the plastic substrate is then evaluated under the illumination of a computer screen, [18].
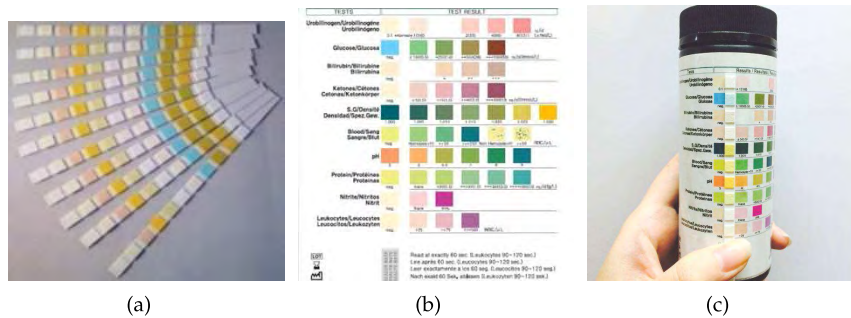
FIGURE 1. Off-the-shelf diagnostic tools for strip-based urinalysis. (a) Urine test strips with multi-analyte sensors. (b) Reference colorimetric sheet where color swatches are arrayed in tabular form, (c) Conventional way of matching the color of reagent pads on the urine test strip.

Among the current technology devices, smartphone is the most promising imaging analytical device for paper-based colorimetric detection, [2], [6], [19]–[30]. The convenience of the embedded built-in cameras and small size of the smartphone makes it stand out as a distinctive alternative to conventional medical devices with spectrometric powers. Employing the use of a smartphone for self-performed urinalysis, Scanadu has launched project Scanaflo [31], which includes a urine test kit and smartphone application. A competing device is uChek, [32], which provides a system for performing strip-based diagnosis using smartphones and other auxiliary equipment. However, technical details of these devices have not been published. In [33], smartphone based mobile instrumentation platform has been proposed for colorimetric diagnosis in pH samples. A change in color is detected via CCD camera of smartphone and evaluated in HSV space with the circular reference array. The colorimetric detection of pH of human sweat and saliva is detected using a smartphone in [34], and additional equipment is required to perform the tests. Recently, another algorithm is proposed for the analysis of colorimetric tests measurements of pH, protein and glucose in [35]. However, the tests require tedious system calibrations, which need to be done carefully, hindering the ease of application. Furthermore, in [36], *seven* urine tests are performed utilizing rectangular urine-strips. Also, Cho et. al. [37], have proposed a microfluidic paper analytical device to serve a low-cost POCT urinalysis to monitor UTI and gonorrhea from human urine. Both Hong and Chang [36] and Cho et al., [37] have studied the effects of light on colorimetric analysis of the test but have not provided the solution to the errors introduced by it.

Even though these applications utilize the current technology as a platform for POCT, the cumbersome setup of the evaluation settings or calibrations and the need for specified diagnostic devices, hinder the practical implementation of these methods for effective POCT use.

In this manuscript, a new urine test strip has been proposed, in which each predetermined composition of interest is arranged in an independent doughnut chart. As for strip-based urinalysis, time is a significant factor that needs to be taken into consideration for the accuracy of results.

After 1 minute when the sample is deposited onto the reagent pads, the color changes in these pads and, lasts for $2\tilde{3}$ minutes. With the proposed strip, named Doughnut-shaped Nearness Urine Tester (DONUT), each composition can be monitored simultaneously as the reference colors in interest are spatially nearby, allowing rapid assessment, with no calibration requirement, making it easy for the end user.

Furthermore, a smartphone-based colorimetric detection algorithm is also developed to transform image data into diagnosis results, without the influence of surrounding illumination conditions. The invariance property of DONUT is contributed by the self-contained configuration of the strip. When the light projected on the strip varies from region to region, the color appearances vary accordingly, preserving the relative differences of the colors. Thus, the proposed framework delivers promising results under various light conditions, allowing it to be readily usable anywhere.

The paper is organized in the following manner: A brief outline of previous works is provided. Followed by the description of the proposed urine tester and its effectiveness over conventional reference array system, along with the proposed colorimetric detection algorithm, in section 2. The results are presented along with the experimental setup in section III, which is followed by the conclusion of the paper.

II. FUNDAMENTALS AND METHODS
A urine test strip consists of porous matrices mixed with dried reagents on a carrier element. The reagent pads interact with liquid in interest and result in color-change due to chemical reactions. Fig. 1 shows an illustration of commercially available urine test strip and the colorimetric reference sheet. The reference system is in tabular form where the reference color swatches, for a chemical element of urine in the analysis, are arrayed in the same row. To obtain a measurable response, the comparison has to be made for each constituent with the corresponding row by finding the reference swatch which best represents the reagent pad in terms of color similarity.

At times, selection of the reference color swatch which best represents a certain constituent is more challenging as some color differences are more difficult to tell apart from another. In these cases, the comparison between possible

reference color swatches with the color of the reagent pad has to be performed back and forth when utilizing conventional reference sheet as shown in Fig. 1(c). On occasions where these swatches necessary for comparison are located spatially far apart, users have no choice but to recall the subtly-varied color gradient of these colors. Consequently, the discomfort in usage due to the configuration of the reference table would likely affect the accuracy of the results.
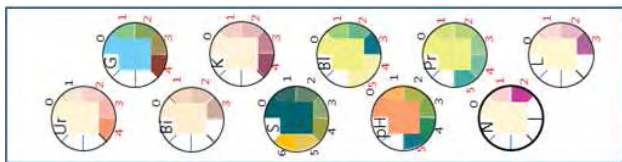

FIGURE 2. Newly proposed urine test strip, Donut-shaped Nearness Urine Tester (DONUT).

A. CONFIGURATION OF DONUT-SHAPED NEARNESS URINE TESTER (DONUT)

The proposed test strip, DONUT is given in Fig. 2. It is designed to analyze the ten predetermined constituents in urine, which are urobilinogen, glucose, bilirubin, ketones, specific gravity, red blood cells (RBC), pH, protein, nitrite, and leukocytes, arranged in two columns. The color swatches for a particular constituent are contained in a doughnut chart where a series of varied hues are distributed accordingly around a square center. The square blocks in the center of these charts are reserved for the corresponding reagent pads. The reference system is further supported by digitized values written with the color swatches.

In a typical analysis process, urine sample is deposited onto all the reagent pads, or, the test strip can be dipped into a sample of interest where excess fluid is blotted off. A sufficient interval is given to ensure that the samples are penetrated and soaked through the reagent pads. A comparison of the color similarities between these pads and the surrounding reference swatches is then made, reflecting the diagnostic results in the form of a value.

While the detection results can be obtained by simple evaluation using the naked eye, the new reference system also supports an alternative to assess the color response of the urine strip using smart-phones.

B. SMARTPHONE-BASED COLORIMETRIC DETECTION

This section introduces a smartphone-based colorimetric detection algorithm in an effort to eliminate the factors of personal subjectivity and surrounding factors.

The interface of the smart-phone application, based on the proposed algorithm, is provided in Fig. 3. The figure demonstrates the interface from image acquisition to the end-result.

The proposed colorimetric algorithm is divided into following main steps:

1) image acquisition
2) circular chart detection
3) segmentation of ROI (Region-Of-Interest)
4) extracting reference and TEST (central swatch of DONUT) color values
5) color comparison and matching of reference colors (of DONUT) with TEST
6) classification of results

The process starts after acquiring an image of the test strip with urine-soaked reagent pads, soaked for about 1 minute, using a smartphone camera within a range of 5 cm to 10 cm, as shown in in Fig. 4. This is followed by detection of the contours of each DONUT chart using Circular Hough Transform [38].

After these circular shapes are successfully detected from the captured image, the region of interest (ROI), corresponding to each reagent pad and the reference color swatches, has to be defined for the purpose of color matching. Even though the color of each separate swatch appears to be the same through visual inspection, Fig. 5(a) clearly illustrates that there are differences in the hue values, especially on the boundaries of each region.

Based on the former observation, ROIs are selected to enclose only a sub-region of the test pads and swatches, excluding the boundaries where the pixel values vary by a greater extent. The ROIs are defined with the geometric information acquired from the preceding step. Specifically, the center of each region is computed and then the width and height of the ROI are calculated with reference to the center. The horizontal and vertical distances of $\frac{R}{4}$ are calculated as the ROI boundaries; where R is the radius of DONUT shape as shown in Fig. 6. For reference swatches, each center is computed at a distance of $(\pm\frac{3R}{4}, \pm\frac{R}{4})$ and $(\pm\frac{R}{4}, \pm\frac{3R}{4})$ from the chart center. The ROIs of these swatches are bounded by the horizontal and vertical distances of $\frac{R}{8}$ from the center. Image description of the segmentation method is shown in Fig. 6.

The differences in intensity values due to the outliers, still present in this dispersed distribution of data, can be filtered using a median filter on ROI before selecting the mean value (of ROI) as the reference value. The color values are then compared to the color value of central test pad, using Matching Factor (MF). An MF in RGB space is calculated by using following:

$$MF_{RGB}(i) = 1 - \left(\frac{\Delta R(i) + \Delta G(i) + \Delta B(i)}{255 \times 3}\right), \quad (1)$$

where, $\Delta R(i) = |R_T - R_i|$, $\Delta G(i) = |G_T - G_i|$, $\Delta B(i) = |B_T - B_i|$, and, $1 \leq i \leq N$ represents the color values in a test and N is the total number of reference color in a given test, computed in previous step, R_i, G_i and B_i; represent the RGB values for each reference color in DONUT array, respectively. MF should be 1 if the colors match perfectly, and 0 if the colors are opposite to each other. The range of ΔR, ΔG ad ΔB is $0 \sim 255$, respectively.

Matching factor for CIE L*a*b*, and HSV color spaces are given as:

$$MF_{LAB}(i) = 1 - \left(\frac{\alpha\Delta L(i) + \beta\Delta a(i) + \beta\Delta b(i)}{(100 + 256 + 256)}\right), \quad (2)$$

FIGURE 3. Developed smart-phone application for Android software using the proposed method. (a) Loading new data. (b) Detecting the strip for urinalysis. (c) Displaying results.
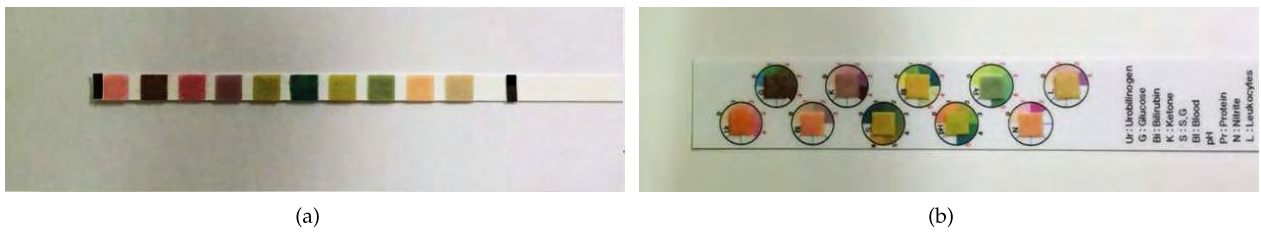

FIGURE 4. Captured images under natural light conditions. (a) Conventional test strip. (b) Proposed test strip.
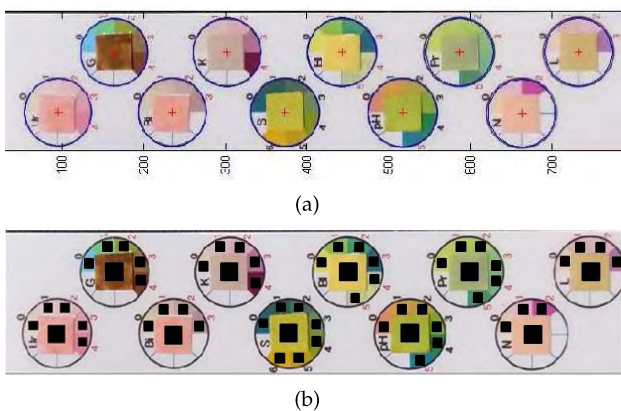

FIGURE 5. (a) Circular Hough Transform. (b) Results of segmentation.

and,

$$MF_{HSV}(i) = 1 - \left(\frac{\alpha \Delta H(i) + \beta \Delta S(i) + \beta \Delta V(i)}{(180 + 100 + 100)} \right). \quad (3)$$

For CIE L*a*b* color space: $\alpha = 0.1634$ and $\beta = 0.418$, and also $0 \leq \Delta L \leq 100$, $0 \leq \Delta a \leq 256$, and, $0 \leq \Delta b \leq 256$;
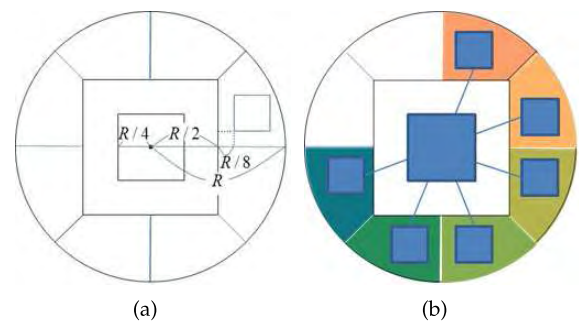

FIGURE 6. Segmentation procedure in DONUT arrays. (a) Partitioning. (b) ROIs of each region.

and for HSV color space: $\alpha = 0.6429$ and $\beta = 0.1786$, and also $0 \leq \Delta H \leq 180$, $0 \leq \Delta S \leq 100$, and, $0 \leq \Delta V \leq 100$.

After calculating the *MF* for each color pad, the best match (BM) is calculated. *BM* is the highest value of all *MF*s, of the center test pad by comparing to the surrounding reference swatch colors, and is given by the following equation:

$$BM = \underset{i}{\operatorname{argmax}}(MF(i)). \quad (4)$$

III. RESULTS AND DISCUSSIONS

This section is divided into two categories. The first comprises the comparison and effectiveness of the proposed DONUT shaped array system over the conventional rectangular arrays. The second provides the detailed analysis of the proposed algorithm as compared to others.

A. EFFECTIVENESS OF DONUT ARRAYS

The goal of the proposed scheme for Smartphone-based colorimetric detection is to ease the user to perform urinalysis while having high accuracy. To compare the performances of the conventional and DONUT reference array system, few experiments are performed. The evaluation method for effects of light on color detection, on both reference arrays, are discussed below. These reference arrays are separately illustrated in Fig. 1 and 2.

The self-shadow effect in image acquisition via smartphone makes the lighting conditions poor. This effect is inevitable during image acquisition. When the conventional strips are used this shadow causes difficulty in matching the color of the test pad with reference array. In case of rectangular arrays, the shadow and illumination, problem is magnified with increasing distance from the test pad.
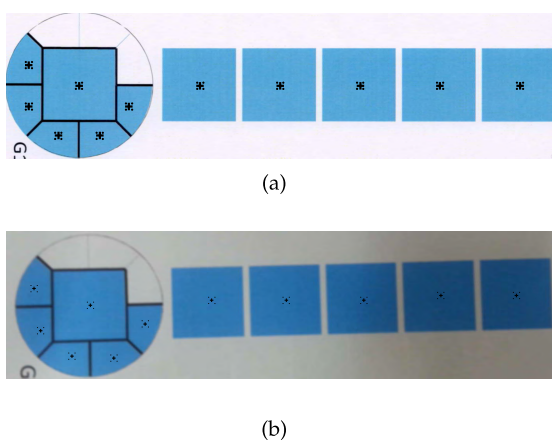

(a)

(b)

FIGURE 7. Glucose Test 1 image (a) scanned image (b) smartphone image.

To show the effectiveness and superiority of the DONUT reference array over the conventional rectangular reference array, a single color array is formed and then color matching is performed, shown in the Fig. 7. The location of reagent pad is taken as the TEST-target and the locations of reference swatches in the arrays are compared to this TEST.

For the experimentation, both reference arrays are printed together and then their image (I) is acquired.

This is followed by choosing a Region of Interest (ROI) of $\omega \times \omega$ pixels for every color reference swatch, as demonstrated in the Fig. 7(a), and Fig. 7(b). There are mostly *five* reference swatches in one urine test (Fig. 4), therefore, for both reference array systems together, there are *eleven* reference swatches in total: *one* is the TEST-target, and *five* for each circular and rectangular reference arrays, respectively.

The image via previous step, is evaluated in RGB, CIE Lab, or HSV color spaces, [39]–[41]. In any of these color space, each reference color will have three *color component* values, thus producing 11×3 images (each with the size of $\omega \times \omega$) in total.

In the fourth step, a surface fitting function is applied to each color component image to remove the noise of each image. This is followed by obtaining the mean value for all *five* colors of circular array and *five* colors of the rectangular array. These mean values are matched with the mean of the test swatch color using a *matching factor* (MF), by utilizing (1) (for RGB). Due to the limited space, this paper only represents the results of RGB space. However, using equations (2) and (3), for the CIE Lab and HSV color spaces, similar results are obtained.

Fig. 8(a) represents the results of the matching factor of the scanned images (Fig. 7(a)) for all the colors of *Glucose test* ($G1 \sim G5$). It is clear from the figure that the results are near to the ideal conditions, when there is no effect of light on the reference colors, the color matching of both the circular and rectangular array with the test swatch is the same.

Fig. 8(b) represents the results of the same analysis for the images obtained by the smartphone camera, and it can be observed from the figure that, when the reference colors are matched with the test swatch, the effect of light on rectangular reference array is more as compared to the circular reference array. The color patch which are further away from the test swatch in the rectangular reference array have less color matching factor, whereas, the colors matching factor for the circular reference array is almost constant (and close to ideal) for all color patches ($1 \sim 5$), as their radial distance from the center of the test swatch is constant. The solid line in both figures represent the mean data for circular (blue line) and rectangular (red line) reference arrays, the dotted (blue and red) lines represent the maximum and minimum of the matching factor for both reference arrays, respectively. In Fig. 8(a) both dotted and solid lines are also very close to each other, representing the compactness of the color matching. Whereas, in Fig. 8(b) the dotted and solid blue line are close, however, the dotted and solid red line drops from the ideal condition (*1* to *0.75* value for dotted and *1* to *0.95* value for the solid, respectively), as the color reference array number increases from *1* to *5*. This phenomenon can be observed for all other urine tests as well.

Fig. 9(a) and 9(b) show the color flow of the Glucose test in RGB space, for scanned image and smartphone image. In Fig. 9(a), the color scheme of all the colors of Glucose Test is compact and close to each other for both DONUT and conventional reference arrays. However, in Fig. 9(b), it can be clearly observed that the color deviation of conventional reference arrays (shown by red line) is greater as compared to the color deviation of DONUT arrays (shown by blue). The color pattern, in both the figures, is different due to the change in illumination. For Fig. 9(a) the pattern of color flow is close to ideal. Whereas, in Fig. 9(b) the color pattern is more close to the darker region of RGB color space.
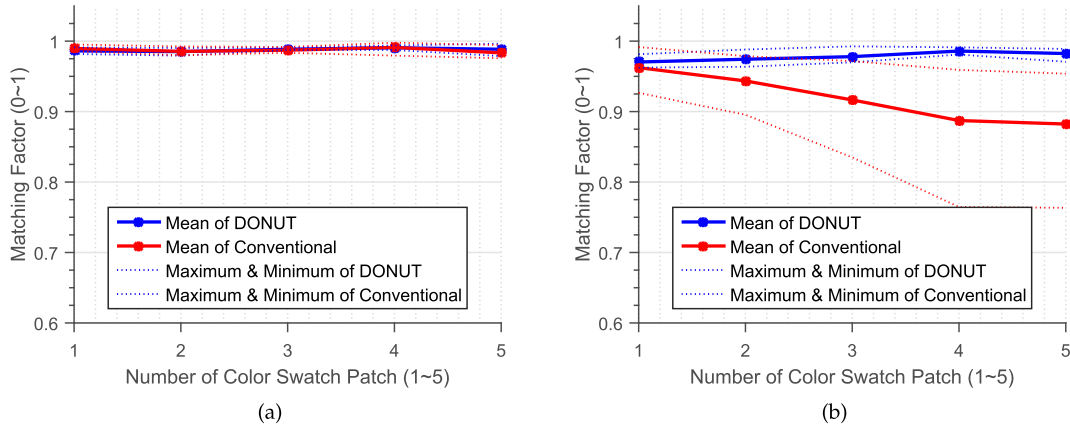
FIGURE 8. Matching factor for Glucose Test 1 for both conventional and the proposed method in RGB color space (a) for scanned image (b) for smartphone image.
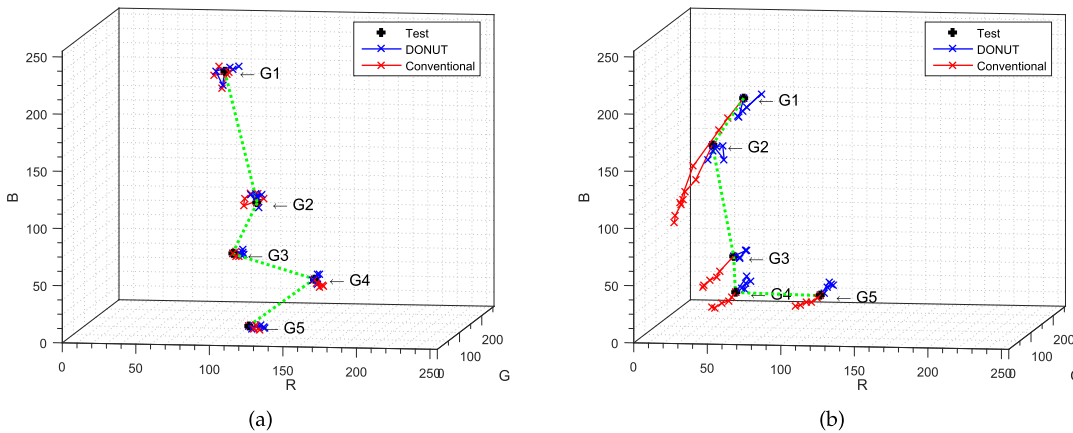

FIGURE 9. Color flow for all colors of Glucose Test for both conventional and proposed strips in RGB color space (a) for scanned image (b) for smartphone image. (The color pattern in both the figures is different due to the illumination change.)

In the Fig. 9(a) and 9(b), the green line represents the connectivity-flow of the colors from $1 \sim 5$.

Fig. 8(a) & 8(b), and Fig. 9(a) & 9(b) confirm the view point that the proposed circular (DONUT) shaped array is less prone to noise caused by the varying light conditions when taking the image from the smartphone, as compared to the rectangular (Conventional) reference array.

The second test uses human vision to compare the effectiveness of the proposed array with conventional array. Under normal room light conditions, 16 participants were asked to evaluate visually the color of test pads, soaked with urine samples, using an assigned array at a time. These participants were chosen among students who did not have color blindness, ranging from 18 to 30 years old. Experiments using conventional and DONUT reference system were separated by three days interval to ensure the integrity of the results. In these experiments, accuracy is achieved when the concentration level of the constituent is same with the ground truth data while precision is evaluated by referring to the standard deviation. A clear comparison of the results can be observed from Fig. 10(a) for a normal urine sample and Fig. 10(b) for an abnormal urine sample. According to these figures,

the new reference systems had considerably small standard deviations in average as compared to the conventional system. These results indicate that decisions of the participants are consistent when they are using the new reference system.

B. EXPERIMENTAL SETUP FOR PROPOSED ALGORITHM ANALYSIS

The test samples used in the experiments are stabilized solutions, composed of urine samples from several individuals, tightly closed and stored at a temperature between $-2\,°C$ to $-6\,°C$. A urine strip reader of model CYBOW Reader 720 is used to obtain the ground truth data before performing the series of experiments. Two smartphones-Samsung Galaxy Note III and I-Phone 5s-are used for image acquisition and processing.

C. PERFORMANCE EVALUATION OF THE PROPOSED ALGORITHM UNDER VARYING ILLUMINATION CONDITIONS

The goal of the second set of experiments is to demonstrate that the performance of the proposed smartphone-based algorithm is also invariant to different illumination conditions.
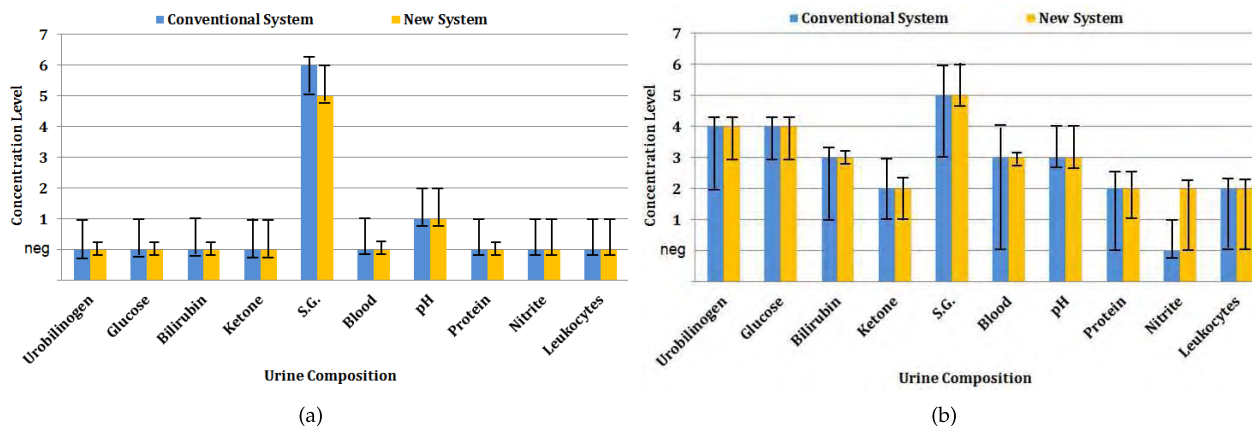
FIGURE 10. Results obtained with the conventional and new reference system. (a) Normal urine test sample. (b) Abnormal urine test sample. Standard deviations are plotted on top of each bar.

TABLE 1. Performances of the proposed algorithm for different smartphones, with different light conditions, for *normal* and *abnormal* urine samples. (Unit: Percentage Rate %)

Composition	Different Light Conditions for iPhone 5s					
	Dim Light		Indoor Light		Outdoor Light	
	Normal	Abnormal	Normal	Abnormal	Normal	Abnormal
Urobilinogen	100	100	100	100	100	100
Glucose	100	100	100	100	100	100
Bilirubin	100	90.0	100	90.0	100	90.0
Ketone	100	100	100	90.0	90.0	90.0
S.G.	100	100	100	100	100	100
Blood	100	100	100	100	100	100
pH	100	100	100	90.0	100	100
Protein	100	100	100	100	100	100
Nitrite	100	90.0	90.0	90.0	90.0	90.0
Leukocytes	90.0	80.0	90.0	80.0	90.0	80.0
	Different Light Conditions for Galaxy Note III					
Urobilinogen	100	100	100	100	100	100
Glucose	100	100	100	100	100	100
Bilirubin	90.0	90.0	90.0	90.0	100	90.0
Ketone	100	80.0	100	80.0	90.0	80.0
S.G.	100	100	100	100	100	100
Blood	100	100	100	100	100	100
pH	90.0	90.0	90.0	90.0	90.0	90.0
Protein	100	100	100	100	100	100
Nitrite	90.0	80.0	90.0	90.0	90.0	90.0
Leukocytes	90.0	90.0	80.0	80.0	90.0	80.0

The color changes of urine reagent pads are examined visually under dim light, room light, and outdoor environments. The experiment procedures are as follows:

1. An image of DONUT array, with urine-soaked test pads, is captured using a smartphone.

2. The diagnostic results of the captured image are evaluated with the inbuilt app on a smartphone and also with MATLAB version 8.0 on a 3.4 GHz Pentium PC.

The images obtained via smartphones are alternated between normal and abnormal urine samples. The experiments are performed 100 times for each smartphone, with one urine test sample at a time in a particular environment. The results are provided in Table 1 and 2.

As per expectations, the results are similar in all environments, as shown in the tables. This is further supported by comparing the results between different smartphone models, where no significant changes are reflected. The slight differences in accuracy rates according to smartphone model systems is due to the fact that different smartphones have different camera specifications.

Ketone, Nitrite, and Leukocytes components showed lower accuracy rates when compared with other constituents.

TABLE 2. Performances of the proposed smartphone based algorithm under different light conditions (even and uneven) as compared to other methods. (Unit: Percentage Rate %)

Composition	Normal Urine Test				Abnormal Urine Test			
	Jong et. al.		Proposed		Jong et. al.		Proposed	
	Even	Uneven	Even	Uneven	Even	Uneven	Even	Uneven
Urobilinogen	96.7	73.3	100	100	90.0	73.3	100	96.7
Glucose	96.7	70.0	100	100	93.3	73.3	100	100
Bilirubin	96.7	86.7	96.7	93.3	93.3	86.7	90.0	86.7
Ketone	93.3	73.3	96.7	96.7	90.0	73.3	96.7	93.3
S.G.	93.3	86.7	100	93.3	93.3	86.7	86.7	90.0
Blood	96.7	96.7	100	100	96.7	86.7	100	96.7
pH	90.0	93.3	90.0	90.0	90.0	86.7	90.0	86.7
Protein	100	76.7	100	100	100	73.3	100	90.0
Nitrite	100	73.3	90.0	86.7	100	73.3	86.7	86.7
Leukocytes	96.7	80.0	90.0	93.3	96.7	76.7	86.7	86.7

The deviations are wide in general regardless of the reference systems used. Therefore, the lower accuracy rates can be ascribed to the reason that these constituents are more challenging to be matched to the right concentration level. However, a good overall outcome with an accuracy rate of 80% and above, revealed the effectiveness of DONUT with the proposed algorithm.

D. PERFORMANCE COMPARISON OF THE PROPOSED ALGORITHM WITH OTHER SMARTPHONE-BASED COLORIMETRIC DETECTION

In this set of experiments, comparisons are made between the proposed and the other smartphone-based approaches. In the work proposed by Jong and Chang [36], black and white markers are placed on both ends of a urine test strip to compensate for the surrounding illumination changes, as shown in Fig. 4. Then, different constituents of the urine sample are evaluated under either H or S channels of HSV color space, and converted into concentration values based on the predetermined calibration curves. The aforementioned method and the proposed smartphone-based algorithm are tested ten times, with Galaxy Note III, under dim, indoor, and outdoor light conditions. The averaged results are shown in Table 2. The experiments are repeated for uneven light conditions, where the strips were shaded partially to make uneven illumination condition. The results are also illustrated in Table 2.

For even light distribution, it can be seen that both systems obtained high accuracy rates. A steep drop in accuracy rates for Jong's method is observed in the experiments with uneven light conditions whereas, the proposed algorithm maintained high performance. This sharp accuracy drop in Jong's method occurred due to the incorrect digitization of black and white markers on both ends of the strip, resulting in the different amount of light spreading on these markers. The proposed smartphone-based algorithm did not suffer from the same drawback due to its self-contained configuration. This design is shown in Fig. 4(b), where light is spread uniformly on

each doughnut chart even when shadow is partly shading the strip. As the relative differences among the reference color arrays and reagent pad remained the same, diagnostic results are correctly computed. Thus, as for the robustness against uneven illumination especially in the presence of shadows, it is shown that the proposed system is suitable for real-life scenarios. This is because the even distribution of light on the surface of the urine test strip cannot be guaranteed in normal circumstances.

IV. CONCLUSION

Point of care testing (POCT) has been integrated into the healthcare system, creating a paradigm shift and offering faster results using portable, easy-to-use devices that can lead to improved patient outcomes. A number of factors, such as demand for development of advanced, faster, and easy-to-use devices are stimulating the demand for POCT. This manuscript aims the development of a new urine test strip along with smartphone-based colorimetric detection algorithm for POCT application. The simplicity, uniqueness, robustness and accuracy of proposed strip and algorithm shall have a great impact on POCT and in general paper based analytical devices.

The experimental results demonstrate that the proposed system is suitable for real-life implementation, whether the detection is performed using naked eye or smartphones. After the process is performed, the diagnostic results can be saved for health monitoring or transmitted immediately to clinical laboratories for professional therapeutic decisions. The independent configuration of DONUT contributes to high performances under varying light conditions, even in the presence of shadows. Thus, it is not only applicable to strip-based urinalysis, but can be widely applied to other strip-based colorimetric detections such as drug strip testing and water quality testing. It is envisioned that these applications can be built on various platforms in the future. This manuscript represents the image analysis in RGB domain; better results are expected if CIE Lab or HSV color space are used.

TABLE 3. Categorical sensitivity and specificity comparison of the proposed algorithm with urinalysis analyzer machine (UAM).

Composition	Category	Actual Concentration Level	Average of UAM	Average of Proposed Method	Categorical sensitivity of Proposed Method	Categorical specificity of Proposed Method
Urobilinogen	Safe	2	2	1.9	100%	100%
	Risk	3	3	3.3	100%	100%
	High	5	5	5.0	100%	100%
Glucose	Safe	2	2	2.1	100%	100%
	Risk	3	3	3.4	100%	100%
	Risk	4	4	4.4	100%	100%
	High	5	5	5.1	100%	100%
	High	6	6	5.2	100%	100%
Bilirubin	Safe	1	2	2.0	100%	100%
	High	5	5	3.9	100%	100%
Ketone	Safe	1	1	1.1	100%	100%
	Risk	3	3	2.2	100%	100%
	High	4	4	3.0	90%	90%
S.G.	Safe	2	2	2.1	100%	100%
	High	4	4	4.5	80%	80%
Blood	Safe	2	2	2	100%	100%
pH	Safe	1	1	1.8	100%	100%
Protein	Safe	1	1	1.1	100%	100%
	Risk	4	4	3.4	90%	80%
	High	6	6	4.1	80%	80%
Nitrite	Safe	1	1	1	100%	100%
Leukocytes	Safe	1	1	1	100%	100%

When using conventional strips, for samples such as urine, blood, or other body fluids, signals are obtained in the form of colors. Evaluation of the changes in colors, which is done by simple human perception, is perceived differently due to varying light conditions, resulting in diagnostic errors which are likely to affect the medical decision-making of users. The main advantage of the proposed strips (DONUT) is robustness against different light conditions even when viewed with naked eye. Besides the DONUT, the proposed smart phone algorithm also have several advantages; such as, no calibration requirements; easy-to-go, compatibility with both Android and iOS based systems, and equivalence in accuracy as compared conditional urine-analysis-machine (UAM). These advantages makes it particularly suitable for early disease detection and patient self-monitoring. Along with these advantages these features also make it more appropriate for quick clinical use.

In future, the improvements can be made in visual perception of the DONUT shape. The compatibility of the DONUST strips and conventional strips for UAM use can be added, which will give another advantage for proposed strips as it could be used for both smartphone and UAM without the hassle of change in equipment. Furthermore, the design of DONUT shape can be improved to incorporate the manufacturing constraints of the urine strips. In addition to this, the proposed algorithm could be further improved for higher accuracy of results. The robustness against noisy conditions can also be added.

APPENDIX
CATEGORICAL SENSITIVITY AND SPECIFICITY COMPARISON OF THE PROPOSED ALGORITHM WITH URINALYSIS ANALYZER MACHINE

This section explains the categorical sensitivity and specificity of the proposed method and compares the results with Urinalysis Analyzer Machine (UAM). For experiments, 300 artificial urine samples prepared using the method described in [42]–[44], are prepared with different concentration levels and are then analyzed via both UAM and the proposed method. The test results of UAM and the proposed method are compared to the actual ground truth of the samples. The categorical sensitivity and specificity of each test using proposed method are also compared with the ground truth data. The results are computed under random light conditions. Also the devices used to carry out the experiments (Galaxy Note III and iPhone 5s) are selected randomly.

Each test is divided into three categories each; namely, safe, risk and high. For example, the glucose test has five

concentration levels, level 1 is categorized as safe, level 2 and 3 are categorized as risk and, 4 and 5 are categorized as high. The measures are used to compare the proposed algorithm with the results of Urine Analyzer Machine; namely–sensitivity (also called the true positive rate), which measures the proportion of positives that are correctly identified for the correct category; and specificity (also called the true negative rate), which measures the proportion of negatives that are correctly identified. Table 3 represents the actual concentration levels, the average measurements using UAM and average measured level using the proposed method. It also shows the categorical sensitivity and specificity of the proposed method. Except for few, most of the results shown have 100% true positive and true negative rates, reflecting the effectiveness of the proposed scheme.

ACKNOWLEDGMENT

REFERENCES

[1] D. Naumann and R. Meyers, *Encyclopedia of Analytical Chemistry*. Chichester, U.K.: Wiley, 2000, pp. 102–131.

[2] L. Shen, J. A. Hagen, and I. Papautsky, "Point-of-care colorimetric detection with a smartphone," *Lab Chip*, vol. 12, no. 21, pp. 4240–4243, 2012.

[3] D. Zhang *et al.*, "Protein detecting with smartphone-controlled electrochemical impedance spectroscopy for point-of-care applications," *Sens. Actuators B, Chem.*, vol. 222, pp. 994–1002, Jan. 2016.

[4] B. M. Cummins, F. S. Ligler, and G. M. Walker, "Point-of-care diagnostics for niche applications," *Biotechnol. Adv.*, vol. 34, no. 3, pp. 161–176, 2016.

[5] S.-C. Liao *et al.*, "Smart cup: A minimally-instrumented, smartphone-based point-of-care molecular diagnostic device," *Sens. Actuators B, Chem.*, vol. 229, pp. 232–238, Jun. 2016.

[6] B. Berg *et al.*, "Cellphone-based hand-held microplate reader for point-of-care testing of enzyme-linked immunosorbent assays," *ACS Nano*, vol. 9, no. 8, pp. 7857–7866, 2015.

[7] S. K. Vashist and J. Luong, "Trends in *in vitro* diagnostics and mobile healthcare," *Biotechnol. Adv.*, vol. 34, no. 3, p. 137, 2016.

[8] S. K. Vashist, P. B. Luppa, L. Y. Yeo, A. Ozcan, and J. H. T. Luong, "Emerging technologies for next-generation point-of-care testing," *Trends Biotechnol.*, vol. 33, no. 11, pp. 692–705, 2015.

[9] L. Kwon, K. Long, Y. Wan, H. Yu, and B. Cunningham, "Medical diagnostics with mobile devices: Comparison of intrinsic and extrinsic sensing," *Biotechnol. Adv.*, vol. 34, no. 3, pp. 291–304, 2016.

[10] D. J. Soldat, P. Barak, and B. J. Lepore, "Microscale colorimetric analysis using a desktop scanner and automated digital image analysis," *J. Chem. Edu.*, vol. 86, no. 5, p. 617, 2009.

[11] E. Kehoe and R. L. Penn, "Introducing colorimetric analysis with camera phones and digital cameras: An activity for high school or general chemistry," *J. Chem. Edu.*, vol. 90, no. 9, pp. 1191–1195, 2013.

[12] T. Schwaebel, O. Trapp, and U. H. Bunz, "Digital photography for the analysis of fluorescence responses," *Chem. Sci.*, vol. 4, no. 1, pp. 273–281, 2013.

[13] E. P. Moraes, M. R. Confessor, and L. H. S. Gasparotto, "Integrating mobile phones into science teaching to help students develop a procedure to evaluate the corrosion rate of iron in simulated seawater," *J. Chem. Edu.*, vol. 92, no. 10, pp. 1696–1699, 2015.

[14] M. Montangero, "Determining the amount of copper(II) ions in a solution using a smartphone," *J. Chem. Edu.*, vol. 92, no. 10, pp. 1759–1762, 2015.

[15] D.-S. Lee, B. G. Jeon, C. Ihm, J.-K. Park, and M. Y. Jung, "A simple and smart telemedicine device for developing regions: A pocket-sized colorimetric reader," *Lab Chip*, vol. 11, pp. 120–126, Nov. 2011.

[16] K. Tohda and M. Gratzl, "Micro-miniature autonomous optical sensor array for monitoring ions and metabolites 1: Design, fabrication, and data analysis," *Anal. Sci.*, vol. 22, no. 3, pp. 383–388, 2006.

[17] A. Lapresta-Fernandez and L. F. Capitán-Vallvey, "Evaluation of analytical reflection scanometry as an analytical tool," *Anal. Methods*, vol. 3, no. 11, pp. 2644–2650, 2011.

[18] D. Filippini and I. Lundstrom, "Measurement strategy and instrumental performance of a computer screen photo-assisted technique for the evaluation of a multi-parameter colorimetric test strip," *Analyst*, vol. 131, pp. 111–117, 2006.

[19] Q. Mei *et al.*, "Smartphone based visual and quantitative assays on upconversional paper sensor," *Biosensors Bioelectron.*, vol. 75, no. 1, pp. 427–432, 2016.

[20] S. Wang *et al.*, "Integration of cell phone imaging with microchip ELISA to detect ovarian cancer he4 biomarker in urine at the point-of-care," *Lab Chip*, vol. 11, no. 20, pp. 3411–3418, 2011.

[21] A. W. Martinez, S. T. Phillips, E. Carrilho, S. W. Thomas, III, H. Sindi, and G. M. Whitesides, "Simple telemedicine for developing regions: Camera phones and paper-based microfluidic devices for real-time, off-site diagnosis," *Anal. Chem.*, vol. 80, no. 10, pp. 3699–3707, 2008.

[22] A. García *et al.*, "Mobile phone platform as portable chemical analyzer," *Sens. Actuators B, Chem.*, vol. 156, no. 1, pp. 350–359, 2011.

[23] K. Choi *et al.*, "Smartphone-based urine reagent strip test in the emergency department," *Telemed. e-Health*, vol. 22, no. 6, pp. 534–540, 2016.

[24] D. Zhang and Q. Liu, "Biosensors and bioelectronics on smartphone for portable biochemical detection," *Biosensors Bioelectron.*, vol. 75, pp. 273–284, Jan. 2016.

[25] J. Hu *et al.*, "Portable microfluidic and smartphone-based devices for monitoring of cardiovascular diseases at the point of care," *Biotechnol. Adv.*, vol. 34, no. 3, pp. 305–320, 2016.

[26] Q. Wei *et al.*, "Fluorescent imaging of single nanoparticles and viruses on a smart phone," *ACS Nano*, vol. 7, no. 10, pp. 9147–9155, 2013.

[27] K. Su *et al.*, "High-sensitive and high-efficient biochemical analysis method using a bionic electronic eye in combination with a smartphone-based colorimetric reader system," *Sens. Actuators B, Chem.*, vol. 216, pp. 134–140, Sep. 2015.

[28] S. K. Vashist, O. Mudanyali, E. M. Schneider, R. Zengerle, and A. Ozcan, "Cellphone-based devices for bioanalytical sciences," *Anal. Bioanal. Chem.*, vol. 406, no. 14, pp. 3263–3277, 2014.

[29] S. K. Vashist, E. M. Schneider, and J. H. T. Luong, "Commercial smartphone-based devices and smart applications for personalized healthcare monitoring and management," *Diagnostics*, vol. 4, no. 3, pp. 104–128, 2014.

[30] S. K. Vashist, T. van Oordt, E. M. Schneider, R. Zengerle, F. von Stetten, and J. H. Luong, "A smartphone-based colorimetric reader for bioanalytical applications using the screen-based bottom illumination provided by gadgets," *Biosensors Bioelectron.*, vol. 67, pp. 248–255, May 2015.

[31] Wikipedia Contributors 'Scanadu'. *Wikipedia the Free Encyclopedia*. Accessed: May 2015. [Online]. Available: https://en.wikipedia.org/wiki/Scanadu

[32] Biosense. (2014). *uchek*. [Online]. Available: http://www.biosense.in/uchek.html

[33] B.-Y. Chang, "Smartphone-based chemistry instrumentation: Digitization of colorimetric measurements," *Bull. Korean Chem. Soc.*, vol. 33, no. 2, pp. 549–552, 2012.

[34] V. Oncescu, D. O'Dell, and D. Erickson, "Smartphone based health accessory for colorimetric detection of biomarkers in sweat and saliva," *Lab Chip*, vol. 13, no. 16, pp. 3232–3238, 2013.

[35] A. K. Yetisen, J. Martínez-Hurtado, A. García-Melendrez, F. da Cruz Vasconcellos, and C. R. Lowe, "A smartphone algorithm with inter-phone repeatability for the analysis of colorimetric tests," *Sens. Actuators B, Chem.*, vol. 196, pp. 156–160, Jun. 2014.

[36] J. I. Hong and B.-Y. Chang, "Development of the smartphone-based colorimetry for multi-analyte sensing arrays," *Lab Chip*, vol. 14, no. 10, pp. 1725–1732, 2014.

[37] S. Cho, T. S. Park, T. G. Nahapetian, and J.-Y. Yoon, "Smartphone-based, sensitive μpad detection of urinary tract infection and gonorrhea," *Biosensors Bioelectron.*, vol. 74, pp. 601–611, Dec. 2015.

[38] S.-C. Pei and J.-H. Horng, "Circular arc detection based on Hough transform," *Pattern Recognit. Lett.*, vol. 16, no. 6, pp. 615–625, 1995.

[39] C. Poynton, *Digital Video and HD: Algorithms and Interfaces*. Amsterdam, The Netherlands: Elsevier, 2012.

[40] R. W. G. Hunt, *The Reproduction of Colour*. Wiley, 2005.

[41] R. S. Hunter, "Photoelectric color difference meter," *J. Opt. Soc. Amer.*, vol. 48, no. 12, pp. 985–993, 1958.

[42] G. Ballman, "Handling infectious materials in the education setting," *Amer. Clin. Lab.*, vol. 8, no. 7, pp. 10–11, 1989.

[43] R. M. Kark, J. R. Lawrence, V. E. Pollak, C. L. Pirani, and R. C. Muehrcke, *A Primer of Urinalysis*, 2nd ed. New York, NY, USA: Hoeber Medical Division, Harper & Row, 1963, p. 27.

[44] J. D. Sharp and D. L. Smailes, "How-to-do-it: A simulation of the blood type test," *Amer. Biol. Teacher*, vol. 51, no. 4, pp. 232–233, 1989.

MOONSOO RA received the B.S. degree in electronics and computer engineering from Hanyang University, Seoul, South Korea, in 2011, where he is currently pursuing the Ph.D. degree. His research interests include machine learning, object detection, video surveillance, and medical image processing.

MANNAN SAEED MUHAMMAD received the M.S. and Ph.D. degrees in mechatronics and information engineering from the Gwangju Institute of Science and Technology, Gwangju, South Korea, in 2006 and 2012, respectively. He is currently with the Sungkyunkwan University, as an Assistant Professor. His research interests include robot vision, image processing, and robots in health-care.

CHIAWEI LIM received the convergence electronics engineering degree from Hanyang University, South Korea, in 2014, where she further continued the master's degree with Video and Image Engineering Laboratory. She was with the Intel Corporation as a System Validation Engineer from 2016 to 2017. She is currently a Deep Learning Engineer with Skymind Corporation. She covers projects, which provide commercial-grade deep learning solutions to business problems. She also supports in developing training materials for deep learning courses.

SEHUI HAN received the M.S. degree in electronics and computer engineering from Hanyang University, Seoul, South Korea, in 2015. He is currently with the LG Electronics as an Image Processing Engineer. His research interests include pattern recognition, object detection, medical image processing, and precise measurement and inspection.

CHANSUNG JUNG received the B.S. degree in electronic engineering from the Korea National University of Transportation, in 2014, and the M.S. degree in intelligent robot engineering from Hanyang University, in 2016. He is currently researching a field of the robot vision in Intelligent Robotics Research Center, Korea Electronics Technology Institute.

WHOI-YUL KIM received the Ph.D. degree in electrical engineering from Purdue University, West Lafayette, IN, USA, in 1989. From 1989 to 1994, he was with the Erik Jonsson School of Engineering and Computer Science, University of Texas at Dallas. He joined Hanyang University in 1994, where he is currently a Professor with the Department of Electronic Engineering. His research interests include health monitoring using mobile devices, visual surveillance, virtual devices, machine vision systems, advanced driver assistance system, and 3-D vision systems in sports, and home appliances.

• • •